



Published in final edited form as:

*Hum Brain Mapp.* 2016 April ; 37(4): 1321–1334. doi:10.1002/hbm.23105.

## The Superficial White Matter in Alzheimer's Disease

Owen Phillips<sup>1,2</sup>, Shantanu H. Joshi<sup>3</sup>, Fabrizio Piras<sup>4</sup>, Maria Donata Orfei<sup>4</sup>, Mariangela Iorio<sup>4</sup>, Katherine L. Narr<sup>3</sup>, David W. Shattuck<sup>3</sup>, Carlo Caltagirone<sup>1,2</sup>, Gianfranco Spalletta<sup>4</sup>, and Margherita Di Paola<sup>1,5,\*</sup>

<sup>1</sup> Clinical and Behavioural Neurology Dept. IRCCS Santa Lucia Foundation, Rome, Italy

<sup>2</sup> Neuroscience Dept. University of Rome "Tor Vergata", Italy

<sup>3</sup> Ahmanson Lovelace Brain Mapping Center, Neurology Dept. UCLA, California, USA

<sup>4</sup> Neuropsychiatry Laboratory, Clinical and Behavioural Neurology Dept. IRCCS Santa Lucia Foundation, Rome, Italy

<sup>5</sup> Human Studies Dept. LUMSA University, Rome, Italy

### Abstract

White matter abnormalities have been shown in the large deep fibers of Alzheimer's disease patients. However, the late myelinating superficial white matter comprised of intracortical myelin and short-range association fibers has not received much attention. In order to investigate this area, we extracted a surface corresponding to the superficial white matter beneath the cortex, and then applied a cortical pattern-matching approach which allowed us to register and subsequently sample diffusivity along thousands of points at the interface between the gray matter and white matter in 44 patients with Alzheimer's disease (Age: 71.02±5.84, 16M/28F) and 47 healthy controls (Age 69.23±4.45, 19M/28F).

In patients we found an overall increase in the axial and radial diffusivity across most of the superficial white matter ( $p < 0.001$ ) with increases in diffusivity of more than 20% in the bilateral parahippocampal regions and the temporal and frontal lobes. Furthermore, diffusivity correlated with the cognitive deficits measured by the Mini-Mental State Examination scores ( $p < 0.001$ ).

The superficial white matter has a unique microstructure and is critical for the integration of multimodal information and during brain maturation and aging. Here we show that there are major abnormalities in patients and the deterioration of these fibers relates to clinical symptoms in Alzheimer's disease.

### Keywords

white matter; intracortical myelin; DTI; interstitial neurons; diffusion; short-range association fibers; U-fibers; oligodendrocytes; neurodegeneration

---

Corresponding Author: Margherita Di Paola Psy.S., PhD. m.dipaola@hsantalucia.it, Santa Lucia Foundation, IRCCS, Via Ardeatina 306 - 00142 Rome (Italy), 0039 - 06 5150 1121.

The Authors have no conflicts of interest to report.

## Introduction

Alzheimer's disease is a neurodegenerative disease that affects much of the brain. There have been numerous investigations into the deleterious effects of the disease on subcortical and cortical gray matter and deep white matter (large easily identifiable early myelinating fibers (for reviews see (Amlie and Fjell, 2014; Jack Jr. and Holtzman, 2013; Weiner et al., 2012)). Almost all of these suggest abnormalities to the cortical gray matter (Ridgway et al., 2012) and the white matter of Alzheimer's disease patients (Sachdev et al., 2013), with both voxel (Matsuda, 2013) and tract-based (Liu et al., 2011) atlasing methods.

The novelty of this study was to focus on the health of the tissue lying at the interface between the cortical gray matter and white matter (here called the superficial white matter). The hypothesis behind this investigation was that the superficial white matter could be sensitive to disease processes because of its location and because of its unique characteristics. Indeed, the superficial white matter is comprised of intracortical myelin and short-range association fibers (U-fibers), which are the last regions to myelinate. This results in high plasticity but also high vulnerability (Bartzokis, 2004). Secondly, the oligodendrocytes in the superficial white matter myelinate many axon segments with fewer wraps than in the deep white matter (Butt and Berry, 2000), which gives them less protection against damage and makes the fibers more sensitive to impairments (Haroutunian et al., 2014). Third, the superficial white matter has a much higher proportion of "interstitial neurons" than the deep white matter (Suarez-Sola et al., 2009), and these neurons have been found to be relevant for the pathogenesis of Alzheimer's disease (van de Nes et al., 2002).

Most of the studies mentioned above, theoretically do not exclude the superficial white matter from their analysis procedures, however, they are limited with regard to the spatial alignment of the cortical boundary, which is highly variable across subjects (Smith et al., 2006; Thompson et al., 2001). Therefore, voxel- or tract-based atlasing methods might lack the sensitivity for quantifying corticocortical connectivity at the juncture between the gray matter and white matter. Similarly, because the white matter tracts in this region have less-defined trajectories, tract-based atlasing methods are limited for extracting these pathways with certainty (Oishi et al., 2008). Likely, because of this the superficial white matter has not received much attention in Alzheimer's disease. However, the superficial white matter is especially vulnerable to the normal aging process (Phillips et al., 2013) and may thus also be vulnerable to disease processes in Alzheimer's disease.

To address if degeneration of the superficial white matter is associated with Alzheimer's disease we first wanted to assess if there was a difference in diffusion MRI metrics of whole brain superficial white matter between patients with Alzheimer's disease and controls. Subsequently we set out to determine the location of these abnormalities, their severity and their role in clinical manifestations. We predicted that diffusivity measures in the superficial white matter would be abnormal in Alzheimer's disease patients and these abnormalities would be most severe in temporal and frontal lobes because they are late myelinating (Phillips et al., 2013) and because the mesial temporal lobe is affected early in the disorder (Braak et al., 1999), and less severe or even absent in the motor cortices because motor

cortices are spared until the late stage of the AD (Braak et al., 1999). Finally, we predicted that these abnormalities would be related to clinical measures of disease severity.

To achieve the goals above, we investigated a sample of 91 subjects (44 Alzheimer's disease patients, 47 healthy controls) by applying an advanced computational analysis approach that combines information from both diffusion and structural MRI data to allow local sampling of superficial white matter integrity measures. This approach, which is highly sensitive for extracting and comparing diffusion tensor imaging (DTI) metrics within the superficial white matter at the juncture of the gray matter and white matter (Phillips et al., 2011; Phillips et al., 2013), was applied to estimate and compare the effects of Alzheimer's disease for axial, radial, mean diffusivity and fractional anisotropy, at thousands of spatially matched locations within the superficial white matter.

## Materials and Methods

### Subjects

We included patients with a diagnosis of mild to moderate Alzheimer's disease who were recruited consecutively in our memory clinic in Rome, Italy. The diagnosis of probable Alzheimer's disease was made by a trained clinical neuropsychiatrist, according to the revised criteria for Alzheimer's disease published by the Alzheimer's Association Research Roundtable (McKhann et al., 2011). We included only drug-free patients with a new diagnosis of Alzheimer's disease, patients who were not undergoing treatment with Acetylcholinesterase inhibitors and had not been treated with psychotropic drugs (i.e. antidepressants, antipsychotics, anxiolytics or mood stabilizers) in the last two years. Inclusion criteria were: 1) the global cognitive impairment, defined as a Mini-Mental State Examination (MMSE) (Folstein et al., 1975) score equal or higher than 10 and a Clinical Dementia Rating (CDR) (Hughes et al., 1982) of 1; 2) vision and hearing sufficient for compliance with testing procedures (eyeglasses and/or hearing aids permissible). Exclusion criteria were: 1) major medical illnesses (e.g., unstabilized diabetes, obstructive pulmonary disease or asthma; hematologic/oncologic disorders; vitamin B12 or folate deficiency, as evidenced by blood concentrations below the lower limits of the reference intervals; pernicious anemia; clinically significant and unstable active gastrointestinal, renal, hepatic, endocrine or cardiovascular system disease; newly treated hypothyroidism); 2) comorbidity of primary psychiatric or neurological disorders (e.g., schizophrenia, mood depression, stroke, Parkinson's disease, seizure disorder, head injury with loss of consciousness) or any other significant mental or neurological disorder; 3) known or suspected history of drug/alcohol dependence and abuse during lifetime; 4) any potential brain abnormalities and microvascular lesions as apparent on conventional T2- and FLAIR-scans; in particular, the presence, severity, and location of vascular lesions were rated by two expert radiologists according to a protocol designed for the Rotterdam Scan Study (Ikram et al., 2011). Generally, they were considered present in cases of hyperintense lesions on both proton-density and T2-weighted (see image acquisition) and rated semiquantitatively as 0 (none), 1 (pencil-thin lining), 2 (smooth halo), or 3 (large confluent) for three separate regions; adjacent to frontal horns (frontal caps), adjacent to the wall of the lateral ventricles (bands), and adjacent to the occipital horns (occipital caps). The total vascular lesion load was

calculated by adding the region-specific scores (range, 0–9). In the present study, only participants rated 0–1 were included; 5) lack of a “reliable” caregiver defined as being able to report to the clinic, fill in the scales for caregivers, ensure compliance with treatment and clinical visits (MRI acquisition, neuropsychological and psychiatric evaluation). For patients included in this study, all patients were able to sign and fill in consent and study materials.

The sociodemographic, clinical, cognitive and functional characteristics of the final clinical sample are summarized in Table 1.

### Ethics Statement

All participants provided written informed consent. Consent was obtained according to the Declaration of Helsinki and the Santa Lucia Foundation Research Ethics Committee approved the study.

### MRI Data Acquisition

All MRI data were acquired on a 3T Allegra MRI system (Siemens, Germany) using a birdcage head coil. Scans were collected in a single session, with the following pulse sequences: 1) T1-weighted 3D images, with partitions acquired in the sagittal plane using a modified driven equilibrium Fourier transform (Deichmann et al., 2004) sequence (TE/TR/TI: 2.4/7.92/910 ms, flip angle: 15°, 1 mm<sup>3</sup> isotropic voxels); and 2) diffusion-weighted volumes were also acquired using SE echo-planar imaging (TE/TR: 89/8500 ms, bandwidth: 2126 Hz/voxel, matrix: 128 × 128, 80 axial slices, voxel size: 1.8 × 1.8 × 1.8 mm) with 30 non-collinear distributed orientations for the diffusion sensitizing gradients at a b value of 1000 s/mm<sup>2</sup> and 6 b = 0 images. Scanning was repeated three times to increase the signal-to-noise ratio.

Images were also visually inspected for movement artifacts; subjects with excessive movement in their scans were excluded.

### Structural MRI Processing

The T1-weighted MRI were corrected for head tilt and alignment using FSL Flirt (<http://fsl.fmrib.ox.ac.uk/fsl/fslwiki/FLIRT>) with a 6-parameter rigid-body transformation. Images were then processed using BrainSuite’s cortical surface extraction pipeline (<http://brainsuite.org/processing/surfaceextraction/>, V15B), which produces surface models of the cerebral cortex from T1 MRI (Shattuck and Leahy, 2002). In brief, BrainSuite performs a sequence of image analysis steps including skull and scalp removal, nonuniformity correction, tissue classification, registration-based identification of the cerebrum, topology correction, and surface generation to produce triangular surface mesh models of the inner and outer boundaries of the cerebral cortex. Next, the surfaces for each subject were registered to a reference atlas surface using BrainSuite’s surface/volume registration software (SVReg; <http://brainsuite.org/processing/svreg/>, V14B) (Joshi et al., 2007). This is a refined cortical pattern matching-procedure that enables cortical surface mapping via alignments between surface features. SVReg first finds a one-to-one map between these surfaces via an intermediate flat map (Joshi et al., 2004). Geodesic curvature flow is used to

improve registration of the sulcal features (Joshi A, Shattuck DW, 2012). This results in a spatial alignment of the white/gray matter cortical surfaces across all subjects.

### DTI Processing

Diffusion-weighted images were first processed with FMRIB's Software Library (FSL 4.1 [www.fmrib.ox.ac.uk/fsl/](http://www.fmrib.ox.ac.uk/fsl/)). Images were corrected for eddy current distortion using FSL's "eddy\_correct". The non-diffusion-weighted images were skull stripped using FSL's Brain Extraction Tool (BET) (<http://www.fmrib.ox.ac.uk/fsl/bet2/index.html>) and used to mask all diffusion-weighted images (Smith, 2002). The output images were then processed with the BrainSuite Diffusion Pipeline (BDP; <http://brainsuite.org/processing/diffusion/>) (Bhushan et al., 2015). This included registration-based distortion correction using a constrained non-rigid registration based on mutual-information. It used the bias-field corrected anatomical image generated by BrainSuite as a registration template to constrain the registration using spatial regularization and physics-based characteristics of distortion in EPI sequences. BDP was used to fit tensor models to the diffusion MRI data, from which diffusion measures (fractional anisotropy, mean diffusivity, radial diffusivity, and axial diffusivity) were computed.

### Mapping the Superficial White Matter: Fig. 1

Details for mapping the superficial white matter contained in (Phillips et al., 2011; Phillips et al., 2013), however, in short, after T1 and DTI processing, a mask was applied to the DTI images with the subcortical gray matter and ventricle labels from BrainSuite (<http://brainsuite.org/processing/svreg/>). This was done to reduce the possible partial volume effects in these regions and further because our focus was not on changes within subcortical structures so removing them reduced the possibility of changes in these structures from influencing the results. No other masking was used. DTI images were then smoothed using a 2-mm kernel. Finally, to allow cross-subject sampling of anatomically comparable superficial white matter axial/radial/mean diffusivity and FA, diffusivity images were sampled along each vertex of the white matter surface (158,748 vertices) using "Image To Shape Attributes" from the LONI Shape Tools (Joshi et al., 2010; Joshi et al., 2012) <http://www.bmap.ucla.edu/portfolio/software/ShapeTools/>. Some important points about the process are worth mentioning, the registration procedure between the DTI and T1 images and has been significantly improved in recent years which allowed us to use a smaller smoothing kernel than in the past (Phillips et al., 2011; Phillips et al., 2013). Furthermore, we had previously (Phillips et al., 2011; Phillips et al., 2013) used a T1 tissue classified image to mask the corresponding DTI images so that only T1 classified white matter was left. However, here we used a subcortical gray matter and ventricle mask. We did not use a T1 classified white matter mask since improved registration between structural and diffusion images significantly reduced the need for smoothing and thus the possible influence of voxels that were completely gray matter. Third, the white matter surface created by BrainSuite is based on the T1 classified image. However, T1 weighted images are not optimized to quantify "myelinated white matter volume" (Haroutunian et al., 2014). This is because tissue segmentation itself, relies on the thresholding signal intensity values for the purpose of classifying brain tissue types, and may also be impacted by microstructural changes in the interface between the gray matter and white matter that occur with age. The

practical result of this is that if we had chosen to apply a T1 WM classified mask as opposed to the ventricle and subcortical gray matter mask that was used; we would reduce the sensitivity of the approach to intracortical myelin. Thus, given the data we had available, our approach optimized sensitivity to diffusivity changes at the juncture of the gray and white matter. However, scans with greater resolution that could give a better estimation of the boundary between the white and gray matter could further improve sensitivity. Furthermore, although the cross registration between the DTI and T1 images has been greatly improved, some misalignment will undoubtedly occur. Again, higher resolution scans could possibly reduce this limitation. Finally, Freesurfer's Tracula (<https://surfer.nmr.mgh.harvard.edu/fswiki/Tracula>) motion correction (dmri\_motion) (Benner et al., 2011; Yendiki et al., 2014) was used to estimate differences in motion correction between patients and controls and an independent samples T-test was used to test for differences between groups.

### Statistical Analysis

Demographic differences were assessed using chi-square, independent sample t-tests or with the General Linear Model as appropriate. Statistical analyses were performed using SPSS 20.0.

Superficial white matter axial/radial/mean diffusivity and fractional anisotropy values were averaged at each vertex point across the white matter surface separately for patients and controls. The whole brain mean value was then extracted. These mean values were then analysed using SPSS's General Linear Model with sex and age as covariates. The p-values were corrected for multiple comparisons using the false discovery rate ( $p=0.05$ ).

DTI measures with high spatial resolution across the superficial white matter surface were analyzed with the General Linear Model (<http://brainsuite.org/bss/>) to test for the effects of disease. Sex and age were included in the model as covariates. Surface based p-values were corrected using a false discovery rate correction ( $p=0.05$ ).

To calculate how much the diffusivity was different at each vertex between groups, percentage change maps were created from the mean surface maps. These calculated the percentage difference at each vertex that the patient group deviated from the control group for axial, radial, mean diffusivity and fractional anisotropy.

To investigate whether superficial white matter changes were related to global index of disease severity, correlation analyses between MMSE and whole brain superficial white matter diffusivity were performed within the patient group. Sex and age were included as covariates.

## Results

### Subject demographics and clinical data (Table 1)

Alzheimer's disease patients and controls did not differ in age or gender **or head motion**. As expected, Alzheimer's disease patients had significantly poorer performances on the MMSE.



### Whole brain superficial white matter findings (Fig. 2 & Fig. 3)

Mean superficial white matter diffusivity values of all vertices across superficial white matter surface are shown in Fig. 2 for patients and controls. Bar graphs in Fig. 3, show the significant effect of Alzheimer's disease on the superficial white matter averaged over the whole brain. Statistical details are outlined in Table 2. Diffusivity measures for whole brain superficial white matter diffusivity were significantly different between patients and controls for all measures. Patients had increased axial, radial, and mean diffusivity and reduced fractional anisotropy compared to controls.

### High Resolution Vertex Based superficial white matter findings (Fig. 4)

Fig. 4 shows the effect of the statistical comparison between Alzheimer's disease and control for superficial white matter axial diffusivity, radial diffusivity, mean diffusivity, and fractional anisotropy at each vertex (high spatial density). Only effects that survived FDR correction are shown.

**Axial, Radial, Mean Diffusivity Findings**—Significant disease related changes in the superficial white matter axial/radial/mean diffusivity were observed in all parts of the brain ( $p < 0.05$ , FDR corrected) (Fig. 4A-C). However, effects were particularly pronounced in both the left and right temporal lobe and parahippocampal region as well as the medial and dorsolateral frontal and prefrontal regions. Because the disease effects covered most of the brain, it is worth highlighting the regions that appear spared from the disease, namely both the left and right motor cortex did not show prominent disease effects. Furthermore, although effects were pronounced in both hemispheres, the left frontal lobe had more widespread changes as did the right insular and occipital lobe compared to the opposing hemisphere. The distribution of disease effects for axial and radial diffusivity were very similar, however, axial effects covered larger and more disperse regions.

**Fractional anisotropy**—Significant fractional anisotropy effects were not observed in the left hemisphere. In the right hemisphere (lower values in patients indicated in blue – Fig. 4D), effects were seen in the posterior portion of the corpus callosum as well as the occipital and medial parietal lobe.

### Percentage Difference in Superficial White Matter Diffusivity (Fig. 5)

Fig. 5 quantifies the results obtained by the previous statistical comparison (see Fig. 4). It shows the vertex based percentage difference between Alzheimer's disease and controls in superficial white matter axial diffusivity, radial diffusivity, mean diffusivity, and fractional anisotropy at high spatial density.

**Axial, Radial, Mean Diffusivity Findings**—There were increases between 5-15% in the superficial white matter axial/radial/mean diffusivity for Alzheimer's disease patients across most of the brain, leaving only the motor cortices spared. The left frontal lobe had increases in diffusivity for patients between 5-20%, this was again similar for the right frontal lobe however, except for the right dorsolateral cortex where diffusivity increases reached 25%. Both the bilateral occipital lobes had increases between 7-20% with the right occipital lobe displaying even greater increases. The bilateral temporal lobes had similar increase,

however, the left temporal lobe, middle temporal, superior temporal and angular gyrus had larger increases ranging from 15 to 25%. Bilaterally, the parahippocampal gyrus had the most extreme increases in diffusivity that ranged from 20 to 30%. These effects were more widespread in the right hemisphere and also were present to a lesser extent in the fusiform gyrus.

**Fractional anisotropy**—There was decreased FA across much of the brain in patients between 5-15% with the greatest reductions in bilateral occipital lobes. Scattered areas showed increased FA in patients that ranged between 5-10%.

### Correlations with MMSE (Fig. 6)

MMSE was significantly correlated with whole brain superficial white matter axial diffusivity ( $r = -0.557$ ,  $P < 0.001$ ), radial diffusivity ( $r = -0.541$ ,  $P < 0.001$ ), and mean diffusivity ( $r = -0.548$ ,  $P < 0.001$ ).

### Supplementary Results: Lobar Disease Effects

*Supplementary Figure 1* shows significant differences in axial diffusivity, radial diffusivity, mean diffusivity, and fractional anisotropy between patients and controls in Lobar Superficial White Matter.

FDR-corrected  $p$  values shown in *Supplementary Table 1* confirm the effects of disease on the diffusivity within the left and right hemisphere and within each of the lobar regions (Frontal, Parietal, Temporal, Occipital, Limbic and Insular). Only fractional anisotropy within the left and right Frontal, Limbic and Insular lobes as well as the left Parietal and right Temporal lobe was not statistically significant.

## Discussion

In this study, we examined the superficial white matter across the whole brain in an Alzheimer's disease and a healthy control sample. Results revealed large increases in whole brain superficial white matter diffusivity in Alzheimer's disease patients compared to controls. These significant findings suggest that abnormalities are pervasive across the whole brain. However to determine whether some regions are more vulnerable, we examined vertex-wise changes over the superficial white matter, which allowed us to pinpoint the disease effects associated with increased diffusivity locally on the brain (see Fig. 4 & 5). These disease effects were significant in most areas of the brain but were particularly prominent bilaterally in the parahippocampal gyrus and the temporal lobes while the motor regions were relatively spared. This pattern appears to be strongly related to the described progression of Alzheimer's disease (Braak et al., 1999).

Finally, we showed significant associations between changes in the axial, radial, and mean superficial white matter diffusivity and the disease severity score (MMSE) in patients.

There are a growing number of studies of white matter in Alzheimer's disease patients. These almost universally point to abnormal deep white matter in Alzheimer's disease patients, with axonal damage proposed as the underlying mechanism together with



decreased and progressive myelination (Di Paola et al., 2010a; Di Paola et al., 2010b); for review see: (Amlien and Fjell, 2014). The present findings expand the literature on brain changes in Alzheimer's disease providing a more comprehensive picture of potential white matter pathology in Alzheimer's disease.

The main reason for this is because the deep white matter and the superficial white matter have different cellular and structural make-up as well as different roles in brain function. Thus, although our findings are in line with the large body of work on the deep white matter, the investigation of the widespread differences between patients and controls in the superficial white matter can suggest different underlying mechanism and provide some clues on this relatively unstudied brain partition.

The cellular make-up of the superficial white matter differs from the deep white matter in several ways. For example, in early myelinating deep white matter, oligodendrocytes tend to myelinate a single axon segment with over 100 myelin membrane wraps, while late-myelinating regions (of which the superficial white matter is part of) contain oligodendrocytes which may myelinate as many as 50 axon segments with fewer than 10 wraps (Butt and Berry, 2000). This makes the late myelinating oligodendrocytes structurally more complex and metabolically overextended (Haroutunian et al., 2014; Peters and Sethares, 2004). While the present study is not directly studying these cells, they are found in high concentrations in the superficial white matter. As such, they could play an important role in the large differences in diffusivity found between patients and controls.

An examination of the vertex-wise changes in the superficial white matter (Fig. 5) suggest that the late myelinating regions such as the language areas as well as the dorsolateral and medial orbital-frontal areas are in fact particularly sensitive compared to early myelinating regions such as the bilateral motor regions. Interestingly, a recent study using cortical myelin maps (Grydeland et al., 2013) (T1w/T2w ratio images sampled along a cortical surface) found a pattern of age effects which is very similar to the disease effects we found. Furthermore, this same pattern was also seen in a separate study using axial and radial diffusivity (Phillips et al., 2013) to investigate age effects in the superficial white matter. These two studies appear to reinforce the hypothesis that late myelinating regions are vulnerable as the brain ages and the current study suggests that this vulnerability is likely even greater in patients with Alzheimer's disease. Indeed we found that the late myelinating superficial white matter such as that in the temporal lobe had increases in diffusivity ranging between ~10-25%.

It's important to note though, that most of the brain had relatively large increases in diffusivity (between ~10-15%), which suggests that all of the superficial white matter is vulnerable to Alzheimer's disease processes with the exception of the motor cortices. The largest increases in diffusivity were seen in the parahippocampal regions with large bilateral increases of greater than 25% in patients compared to controls. It would be easy to disregard the magnitude of this finding as the result of partial volume effects due to the expanded ventricles from reduced hippocampal volume in patients; however, we removed both the ventricles and the hippocampus, thus reducing the likelihood of this. Furthermore, our finding is in line with histological studies which found that the parahippocampal gyrus is

one of the first areas to show neuropathological changes (Braak et al., 1999; Braak and Braak, 1990). Also, volumetric reduction of the parahippocampal gyrus has been reported in MRI studies of mild cognitive impairment and Alzheimer's disease patients (Echávarri et al., 2011) as well as reduced myelination (Fornari et al., 2012). While we don't know the precise biological processes underlying variations in DTI parameters (for review see: (Jones et al., 2012) and caution should be used in interpreting the results, these large increases in diffusivity strongly suggest changes in superficial white matter tissue structure. Furthermore, there is a general agreement that increased mean diffusivity value reflecting greater diffusion of water molecules are associated with tissue atrophy. Increased axial diffusivity is related to white matter axonal changes likely associated with Wallerian degeneration but may also be associated with an increased fiber organization during the human brain tissue life span (Hasan et al., 2007). Increased radial diffusivity is thought to reflect reductions in myelination (Schmierer et al., 2008). Decreased fractional anisotropy indicates the loss of water directionality likely due to damage of the structural organization of the tissue. It's worth highlighting that axial, radial and mean diffusivity were much more sensitive to disease processes than fractional anisotropy. This is likely because in the superficial white matter, the difference between axial and radial diffusivity values is smaller than in the deep white matter, this suppresses the usefulness of fractional anisotropy as a measure in this region. Thus, our findings in Alzheimer's disease patients tentatively suggest that the superficial white matter incurs axonal atrophy (increased axial diffusivity) and myelin damage (increased radial diffusivity). In support of this conclusion, one recent study using a ROI approach examined the superficial white matter in a small cohort of Alzheimer's disease patients with magnetization transfer ratio and found bilateral demyelination in a pattern similar to the one presented here in Fig 4 (Fornari et al., 2012).

The correlation between superficial white matter and global disease severity (MMSE), suggests that the structural abnormalities can be seen as a manifestation of the pathologies' evolution. Indeed, superficial white matter has a role in phase synchronization and neuronal synchrony, which is critical for optimized brain function (Grydeland et al., 2013). Thus disruptions to the superficial white matter may lead to disruptions in the propagation of signals across the brain. As indicated by low MMSE scores, Alzheimer's disease patients' brains are not functioning optimally. Our finding of a strong negative correlation between MMSE and diffusivity lends support to this conclusion.

These data is in agreement with a number of EEG studies which have found signal changes in Alzheimer's disease patients (Czigler et al., 2008; Gallego-Jutglà et al., 2014; Jeong, 2004), as well as a recent DTI study looking at abnormalities in short-range fibers in Alzheimer's disease (Gao et al., 2014) that found that the abnormalities contribute to lower cognitive efficiency and higher compensatory brain activation.

Another aspect to point out in the attempt to understand the role of superficial white matter in Alzheimer's disease is that the-superficial white matter contains a large numbers of interstitial neurons. These morphologically heterogeneous cells are numerous in the white matter underlying the cortical gyri and decrease in density towards the deep white matter. Their function is not well known, which may be because they are uniquely represented in humans and only rudimentarily represented in non-primate mammals (for review see:

(Suarez-Sola et al., 2009)). Friedlander MJ and Torres-Reveron J (2009) found that these cells receive excitatory and inhibitory synaptic inputs, potentially monitoring outputs from axon collaterals of cortical efferents, from cortical afferents and/or from each other. These cells therefore participate in modulating functions of local synaptic networks. They have recently been suggested to have played a critical role in the evolution cognition, self-awareness, and human language (Judaš et al., 2013). It's important to note, we cannot yet discern whether or not the interstitial neurons are in anyway damaged in the Alzheimer's disease pathology. However, we have shown that there are significant abnormalities in the tissue where they reside in high numbers. If the interstitial neurons function is as important as the emerging research suggests it is, further investigations into the interstitial neurons is warranted.

## Limitations

Some potential study limitations are worth noting. As discussed in the methods section, partial volume effects are a potential problem as they are with any method that uses segmentation and steps were taken to minimize this confound. Further, the superficial white matter surface is generated from the T1 image, which is not optimised to classify white and gray matter. Future studies could benefit from advanced imaging methods, which could possibly help delineate the boundary at the juncture between the gray matter and white matter. A secondary option would be to generate a superficial white matter surface from the diffusion data directly, which would eliminate the need to register the diffusion data to the T1 image, however, this approach would present its own challenges. Regarding the results, although the disease effects are likely driven by changes in the superficial white matter, there are, as we mention earlier, well documented changes in the deep white matter (Di Paola et al., 2010b) and thus these changes may influence the results. Future studies with high field MRI could help elucidate the relationship between the deep and superficial white matter. Further, we are unable to resolve the important question of whether deficits in structural connectivity contribute to the onset of Alzheimer's disease or whether it is a secondary effect brought on by changes in gray matter. Future longitudinal studies could help clarify this as well as illuminate the role of interstitial neurons. Finally, although DTI protocols with more diffusion directions might be optimal in some contexts, the 30-direction protocol employed in this study included three averages, which serves to increase signal to noise. Thus, this protocol is much superior to a 30-direction protocol including only one average, and no bias is expected with regard to the statistical findings because DTI parameter estimates are the same for both groups. Nonetheless, future studies including higher angular resolution DTI data might help confirm the regional specificity of superficial white matter disconnectivity in Alzheimer's disease and clarify relationships with specific functional impairments.

## Conclusion

The superficial white matter is uniquely complex in humans and continues to myelinate much later in life than any other primate. Given the distinctive cellular makeup, the superficial white matter likely plays an important role in Alzheimer's disease. To support this conclusion, we have demonstrated that it is damaged across most of the brain in

Alzheimer's disease and is associated with Alzheimer's disease-related cognitive impairment.

## Supplementary Material

Refer to Web version on PubMed Central for supplementary material.

## Acknowledgements

This work was supported by the Italian Ministry of Health (IMA) grants: 204/GR-2009-1606835; and RC 10-11-12-13/A.

## References

- Amlien IK, Fjell AM. Diffusion tensor imaging of white matter degeneration in Alzheimer's disease and mild cognitive impairment. *Neuroscience*. 2014; 276C:206–215. <http://www.ncbi.nlm.nih.gov/pubmed/24583036>.
- Bartzokis G. Age-related myelin breakdown: a developmental model of cognitive decline and Alzheimer's disease. *Neurobiol Aging*. 2004; 25:5–62. <http://www.ncbi.nlm.nih.gov/pubmed/14675724>. [PubMed: 14675724]
- Benner T, van der Kouwe AJW, Sorensen AG. Diffusion imaging with prospective motion correction and reacquisition. *Magn Reson Med*. 2011; 66:154–67. <http://www.pubmedcentral.nih.gov/articlerender.fcgi?artid=3121006&tool=pmcentrez&rendertype=abstract>. [PubMed: 21695721]
- Bhushan C, Haldar JP, Choi S, Joshi AA, Shattuck DW, Leahy RM. Co-registration and distortion correction of diffusion and anatomical images based on inverse contrast normalization. *Neuroimage*. 2015; 115:269–280. <http://www.sciencedirect.com/science/article/pii/S1053811915002451>. [PubMed: 25827811]
- Braak E, Griffing K, Arai K, Bohl J, Bratzke H, Braak H. Neuropathology of Alzheimer's disease: what is new since A. Alzheimer? *Eur Arch Psychiatry Clin Neurosci*. 1999; 249(Suppl):14–22. <http://www.ncbi.nlm.nih.gov/pubmed/10654095>.
- Braak H, Braak E. Neurofibrillary changes confined to the entorhinal region and an abundance of cortical amyloid in cases of presenile and senile dementia. *Acta Neuropathol*. 1990; 80:479–486. [PubMed: 2251904]
- Butt AM, Berry M. Oligodendrocytes and the control of myelination in vivo: new insights from the rat anterior medullary velum. *J Neurosci Res*. 2000; 59:477–488. <http://www.ncbi.nlm.nih.gov/pubmed/10679786>. [PubMed: 10679786]
- Czigler B, Csikós D, Hidasi Z, Anna Gaál Z, Csibri E, Kiss E, Salacz P, Molnár M. Quantitative EEG in early Alzheimer's disease patients - power spectrum and complexity features. *Int J Psychophysiol*. 2008; 68:75–80. [PubMed: 18093675]
- Deichmann R, Schwarzbauer C, Turner R. Optimisation of the 3D MDEFT sequence for anatomical brain imaging: technical implications at 1.5 and 3 T. *Neuroimage*. 2004; 21:757–767. <http://www.ncbi.nlm.nih.gov/pubmed/14980579>. [PubMed: 14980579]
- Echávvarri C, Aalten P, Uylings HBM, Jacobs HIL, Visser PJ, Gronenschild EHB, Verhey FRJ, Burgmans S. Atrophy in the parahippocampal gyrus as an early biomarker of alzheimer's disease. *Brain Struct Funct*. 2011; 215:265–271. [PubMed: 20957494]
- Folstein MF, Folstein SE, McHugh PR. Mini-mental state. *Journal of Psychiatric Research*. 1975
- Fornari E, Maeder P, Meuli R, Ghika J, Knyazeva MG. Demyelination of superficial white matter in early Alzheimer's disease: a magnetization transfer imaging study. *Neurobiol Aging*. 2012; 33(428):e7–19. <http://www.ncbi.nlm.nih.gov/pubmed/21190758>.
- Friedlander MJ, Torres-Reveron J. The changing roles of neurons in the cortical subplate. *Front Neuroanat*. 2009; 3:15. [PubMed: 19688111]

- Gallego-Jutglà, E.; Solé-Casals, J.; Vialatte, F-B.; Dauwels, J.; Cichocki, A. A Theta-Band EEG Based Index for Early Diagnosis of Alzheimer's Disease. *J Alzheimers Dis.* 2014. <http://www.ncbi.nlm.nih.gov/pubmed/25147104>
- Gao J, Cheung RT, Chan YS, Chu LW, Mak HK, Lee TM. The relevance of short-range fibers to cognitive efficiency and brain activation in aging and dementia. *PLoS One.* 2014; 9:e90307. <http://www.ncbi.nlm.nih.gov/pubmed/24694731>. [PubMed: 24694731]
- Grydeland H, Walhovd KB, Tamnes CK, Westlye LT, Fjell AM. Intracortical myelin links with performance variability across the human lifespan: results from T1- and T2-weighted MRI myelin mapping and diffusion tensor imaging. *J Neurosci.* 2013; 33:18618–18630. <http://www.ncbi.nlm.nih.gov/pubmed/24259583>. [PubMed: 24259583]
- Haroutunian V, Katsel P, Roussos P, Davis KL, Altschuler LL, Bartzokis G. Myelination, oligodendrocytes, and serious mental illness. *Glia.* 2014; 62:1856–1877. <http://www.ncbi.nlm.nih.gov/pubmed/25056210>. [PubMed: 25056210]
- Hasan KM, Sankar A, Halphen C, Kramer LA, Brandt ME, Juranek J, Cirino PT, Fletcher JM, Papanicolaou AC, Ewing-Cobbs L. Development and organization of the human brain tissue compartments across the lifespan using diffusion tensor imaging. *Neuroreport.* 2007; 18:1735–1739. <http://www.ncbi.nlm.nih.gov/pubmed/17921878>. [PubMed: 17921878]
- Hughes CP, Berg L, Danziger WL. A new clinical scale for the staging of dementia. *Br J Psychiatry.* 1982; 140:566–572. [PubMed: 7104545]
- Ikram MA, Van Der Lugt A, Niessen WJ, Krestin GP, Koudstaal PJ, Hofman A, Breteler MMB, Vernooij MW. The Rotterdam Scan Study: Design and update up to 2012. *Eur J Epidemiol.* 2011; 26:811–824. [PubMed: 22002080]
- Jack CR Jr. Holtzman DM. Biomarker modeling of Alzheimer's disease. *Neuron.* 2013; 80:1347–1358. <http://www.ncbi.nlm.nih.gov/pubmed/24360540>. [PubMed: 24360540]
- Jeong J. EEG dynamics in patients with Alzheimer's disease. *Clinical Neurophysiology.* 2004
- Jones, DK.; Knosche, TR.; Turner, R. White matter integrity, fiber count, and other fallacies: The do's and don'ts of diffusion MRI. *Neuroimage.* 2012. <http://www.ncbi.nlm.nih.gov/pubmed/22846632>
- Joshi, A.; Shattuck, DW. A Fast and Accurate Method for Automated Cortical Surface Registration and Labeling; Fifth Workshop on Biomedical Image Registration; Nashville, Tennessee. 2012. LR
- Joshi, AA.; Shattuck, DW.; Thompson, PM.; Leahy, RM. Cortical surface parameterization by p-harmonic energy minimization; 2nd IEEE Int Symp Biomed Imaging Nano to Macro (IEEE Cat No 04EX821); 2004. 2004.
- Joshi AA, Shattuck DW, Thompson PM, Leahy RM. Surface-constrained volumetric brain registration using harmonic mappings. *IEEE Trans Med Imaging.* 2007; 26:1657–1668. [PubMed: 18092736]
- Joshi SH, Cabeen RP, Joshi AA, Sun B, Dinov I, Narr KL, Toga AW, Woods RP. Diffeomorphic sulcal shape analysis on the cortex. *IEEE Trans Med Imaging.* 2012; 31:1195–1212. <http://www.ncbi.nlm.nih.gov/pubmed/22328177>. [PubMed: 22328177]
- Joshi SH, Cabeen RP, Sun B, Joshi AA, Gutman B, Zamanyan A, Chakrapani S, Dinov I, Woods RP, Toga AW. Cortical sulcal atlas construction using a diffeomorphic mapping approach. *Med Image Comput Assist Interv.* 2010; 13:357–366. <http://www.ncbi.nlm.nih.gov/pubmed/20879251>. [PubMed: 20879251]
- Judaš M, Sedmak G, Kostovi I. The significance of the subplate for evolution and developmental plasticity of the human brain. *Front Hum Neurosci.* 2013; 7:423. <http://www.pubmedcentral.nih.gov/articlerender.fcgi?artid=3731572&tool=pmcentrez&rendertype=abstract>. [PubMed: 23935575]
- Liu Y, Spulber G, Lehtimäki KK, Könönen M, Hallikainen I, Gröhn H, Kivipelto M, Hallikainen M, Vanninen R, Soininen H. Diffusion tensor imaging and Tract-Based Spatial Statistics in Alzheimer's disease and mild cognitive impairment. *Neurobiol Aging.* 2011; 32:1558–1571. [PubMed: 19913331]
- Matsuda H. Voxel-based Morphometry of Brain MRI in Normal Aging and Alzheimer's Disease. *Aging Dis.* 2013; 4:29–37. <http://www.pubmedcentral.nih.gov/articlerender.fcgi?artid=3570139&tool=pmcentrez&rendertype=abstract>. [PubMed: 23423504]
- McKhann GM, Knopman DS, Chertkow H, Hyman BT, Jack CR, Kawas CH, Klunk WE, Koroshetz WJ, Manly JJ, Mayeux R, Mohs RC, Morris JC, Rossor MN, Scheltens P, Carrillo MC, Thies B,

- Weintraub S, Phelps CH. The diagnosis of dementia due to Alzheimer's disease: Recommendations from the National Institute on Aging-Alzheimer's Association workgroups on diagnostic guidelines for Alzheimer's disease. *Alzheimer's and Dementia*. 2011
- van de Nes JAP, Sandmann-Keil D, Braak H. Interstitial cells subjacent to the entorhinal region expressing somatostatin-28 immunoreactivity are susceptible to development of Alzheimer's disease-related cytoskeletal changes. *Acta Neuropathol*. 2002; 104:351–356. [PubMed: 12200620]
- Oishi K, Zilles K, Amunts K, Faria A, Jiang H, Li X, Akhter K, Hua K, Woods R, Toga AW, Pike GB, Rosa-Neto P, Evans A, Zhang J, Huang H, Miller MI, van Zijl PC, Mazziotta J, Mori S. Human brain white matter atlas: identification and assignment of common anatomical structures in superficial white matter. *Neuroimage*. 2008; 43:447–457. <http://www.ncbi.nlm.nih.gov/pubmed/18692144>. [PubMed: 18692144]
- Di Paola M, Luders E, Di Iulio F, Cherubini A, Passafiume D, Thompson PM, Caltagirone C, Toga AW, Spalletta G. Callosal atrophy in mild cognitive impairment and Alzheimer's disease: different effects in different stages. *Neuroimage*. 2010a; 49:141–149. <http://www.ncbi.nlm.nih.gov/pubmed/19643188>. [PubMed: 19643188]
- Di Paola M, Di Iulio F, Cherubini A, Blundo C, Casini AR, Sancesario G, Passafiume D, Caltagirone C, Spalletta G. When, where, and how the corpus callosum changes in MCI and AD: A multimodal MRI study. *Neurology*. 2010b; 74:1136–1142. [PubMed: 20368633]
- Peters A, Sethares C. Oligodendrocytes, their progenitors and other neuroglial cells in the aging primate cerebral cortex. *Cereb Cortex*. 2004; 14:995–1007. <http://www.ncbi.nlm.nih.gov/pubmed/15115733>. [PubMed: 15115733]
- Phillips OR, Clark KA, Luders E, Azhir R, Joshi SH, Woods RP, Mazziotta JC, Toga AW, Narr KL. Superficial white matter: effects of age, sex, and hemisphere. *Brain Connect*. 2013; 3:146–159. <http://www.ncbi.nlm.nih.gov/pubmed/23461767>. [PubMed: 23461767]
- Phillips OR, Nuechterlein KH, Asarnow RF, Clark KA, Cabeen R, Yang Y, Woods RP, Toga AW, Narr KL. Mapping corticocortical structural integrity in schizophrenia and effects of genetic liability. *Biol Psychiatry*. 2011; 70:680–689. <http://www.ncbi.nlm.nih.gov/pubmed/21571255>. [PubMed: 21571255]
- Ridgway GR, Lehmann M, Barnes J, Rohrer JD, Warren JD, Crutch SJ, Fox NC. Early-onset Alzheimer disease clinical variants: Multivariate analyses of cortical thickness. *Neurology*. 2012; 79:80–84. [PubMed: 22722624]
- Sachdev PS, Zhuang L, Braidy N, Wen W. Is Alzheimer's a disease of the white matter? *Curr Opin Psychiatry*. 2013; 26:244–251. <http://www.ncbi.nlm.nih.gov/pubmed/23493128>. [PubMed: 23493128]
- Schmierer K, Wheeler-Kingshott CA, Tozer DJ, Boulby PA, Parkes HG, Yousry TA, Scaravilli F, Barker GJ, Tofts PS, Miller DH. Quantitative magnetic resonance of postmortem multiple sclerosis brain before and after fixation. *Magn Reson Med*. 2008; 59:268–277. <http://www.ncbi.nlm.nih.gov/pubmed/18228601>. [PubMed: 18228601]
- Smith SM. Fast robust automated brain extraction. *Hum Brain Mapp*. 2002; 17:143–155. <http://www.ncbi.nlm.nih.gov/pubmed/12391568>. [PubMed: 12391568]
- Smith SM, Jenkinson M, Johansen-Berg H, Rueckert D, Nichols TE, Mackay CE, Watkins KE, Ciccarelli O, Cader MZ, Matthews PM, Behrens TE. Tract-based spatial statistics: voxelwise analysis of multi-subject diffusion data. *Neuroimage*. 2006; 31:1487–1505. <http://www.ncbi.nlm.nih.gov/pubmed/16624579>. [PubMed: 16624579]
- Suarez-Sola ML, Gonzalez-Delgado FJ, Pueyo-Morlans M, Medina-Bolivar OC, Hernandez-Acosta NC, Gonzalez-Gomez M, Meyer G. Neurons in the white matter of the adult human neocortex. *Front Neuroanat*. 2009; 3:7. <http://www.ncbi.nlm.nih.gov/pubmed/19543540>. [PubMed: 19543540]
- Thompson PM, Vidal C, Giedd JN, Gochman P, Blumenthal J, Nicolson R, Toga AW, Rapoport JL. Mapping adolescent brain change reveals dynamic wave of accelerated gray matter loss in very early-onset schizophrenia. *Proc Natl Acad Sci U S A*. 2001; 98:11650–11655. <http://www.ncbi.nlm.nih.gov/pubmed/11573002>. [PubMed: 11573002]
- Weiner MW, Veitch DP, Aisen PS, Beckett LA, Cairns NJ, Green RC, Harvey D, Jack CR, Jagust W, Liu E, Morris JC, Petersen RC, Saykin AJ, Schmidt ME, Shaw L, Siuciak J a, Soares H, Toga AW, Trojanowski JQ. The Alzheimer's Disease Neuroimaging Initiative: a review of papers published



since its inception. *Alzheimers Dement*. 2012; 8:S1–68. <http://www.ncbi.nlm.nih.gov/pubmed/22047634>/<http://www.pubmedcentral.nih.gov/articlerender.fcgi?artid=3329969&tool=pmcentrez&rendertype=abstract>. [PubMed: 22047634]

Yendiki A, Koldewyn K, Kakunoori S, Kanwisher N, Fischl B. Spurious group differences due to head motion in a diffusion MRI study. *Neuroimage*. 2014; 88:79–90. <http://dx.doi.org/10.1016/j.neuroimage.2013.11.027>. [PubMed: 24269273]

Author Manuscript

Author Manuscript

Author Manuscript

Author Manuscript

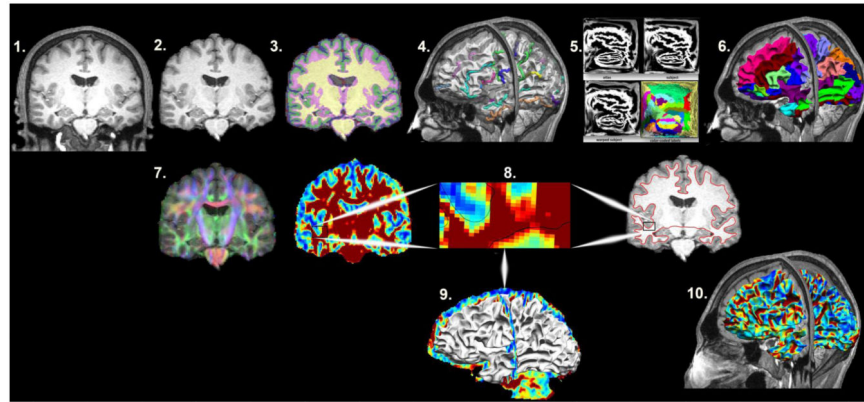


**Fig. 1. Mapping the Superficial White Matter**

Legend. Processing Steps in order to map the superficial white matter. 1. Original T1 structural image. 2. Bias field correction and skull stripping. 3. Tissue classification. 4. Surface extraction and sulcal line drawing. 5. Spatial alignment to the atlas. 6. Region of Interest surface labeling. 7. Distortion correction and co-registration of the diffusion image to the structural MRI image. 8. FA and T1 images with zoom to show the surface boundary. 9. Superficial white matter spatially aligned surface and the FA image allows sampling of diffusivity values at each vertex of the surface. 10. Superficial white matter spatially aligned surface with FA estimated at each vertex. FA = Fractional Anisotropy.

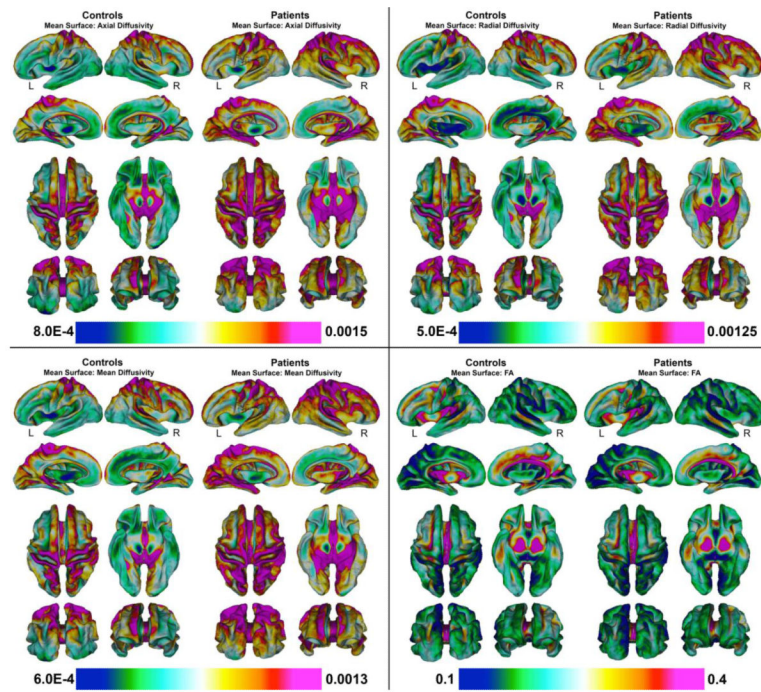


**Fig. 2. Mean superficial white matter for Patients and Controls**  
 Legend. Mean superficial white matter for patients and controls mapped at high-spatial resolution at thousands of homologous locations within the superficial white matter (Axial/Radial/MD Mean units:  $10^{-3} \text{ mm}^2/\text{s}$ ).

Controls.

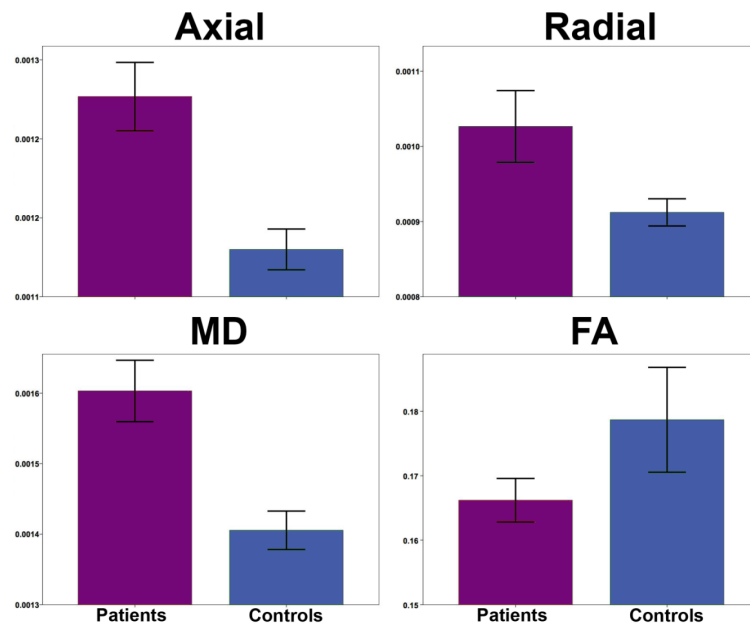


**Fig. 3. Bar Graphs for Average superficial white matter for Patients and Controls**

Legend. Bar graphs show significant differences between average superficial white matter Axial, Radial, Mean diffusivity and FA. The error bars represent the Standard Error Mean (SEM). Legend. Axial = Axial Diffusivity; Radial = Radial Diffusivity; MD = Mean Diffusivity; FA = Fractional Anisotropy (Axial/Radial/MD Mean units:  $10^{-3} \text{ mm}^2/\text{s}$ .)

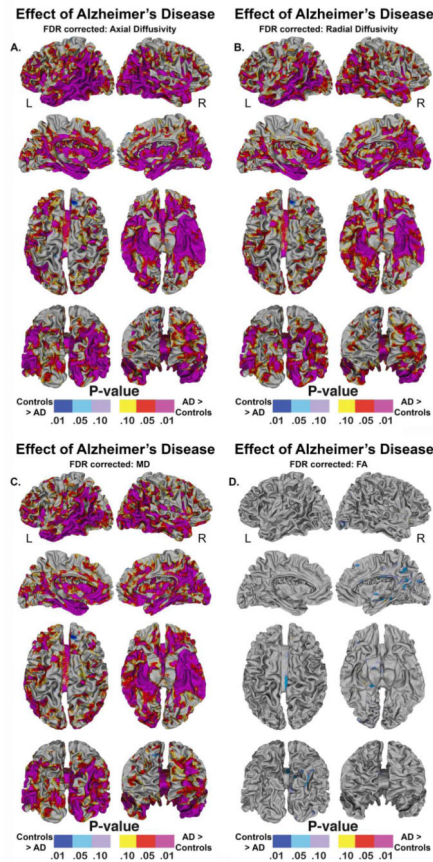


**Fig. 4. Vertex Based Superficial White Matter Findings**

Legend. Probability maps showing effects of Alzheimer’s disease on the superficial white matter (A) Axial Diffusivity, (B) Radial Diffusivity, (C), Mean Diffusivity, (D), Fractional Anisotropy, controlling for age and gender mapped at high-spatial resolution at thousands of homologous locations within the superficial white matter. The direction of effects are indicated by the color bar. For (A-C), red indicates increased diffusivity with disease and blue indicates reduced diffusivity with disease. For (D), blue indicates lower fractional anisotropy with disease and red indicated higher fractional anisotropy with disease.

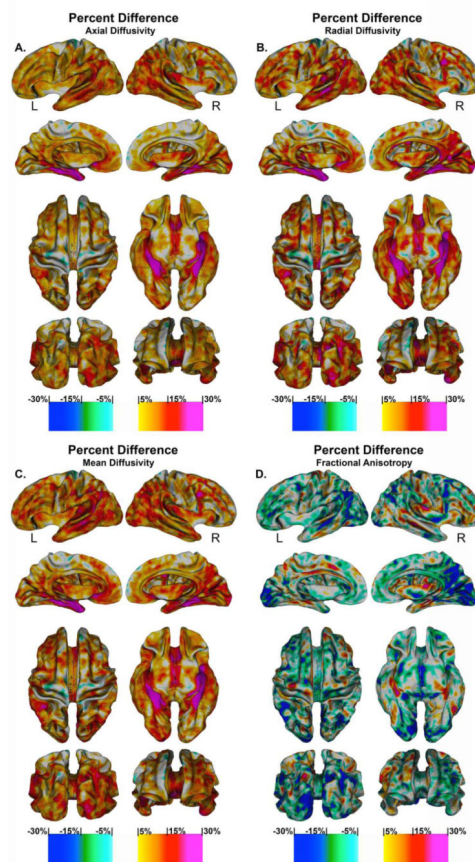


**Fig. 5. Percentage Change in Superficial White Matter Diffusivity**

High-resolution vertex based percentage change maps show the change between Controls and Alzheimer's disease patient's superficial white matter axial diffusivity at high spatial density. Red colours indicate the percentage diffusivity increased with disease while the blue colours indicated the percentage diffusivity decreased with disease.



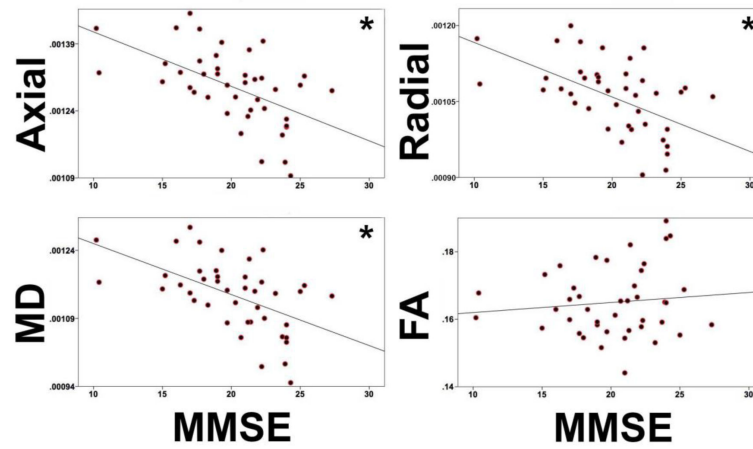


**Fig. 6. MMSE and Whole Brain Diffusivity Correlations**

Legend. \* Indicates a significant correlation between MMSE and diffusivity parameters. FA = Fractional Anisotropy; Axial = Axial Diffusivity; Radial = Radial Diffusivity. MD = Mean Diffusivity. (Axial/Radial/MD Mean units: 10–3 mm<sup>2</sup>/s.)

**Table 1**

Sociodemographic and clinical characteristics of patients and control subjects

Characteristics	Controls (n=47)	AD (n=44)	Fisher's Exact Test; or T Test	df	P values
Gender male/female	19/28	16/28	-0.35	89	0.69
Age years $\pm$ SD	69.23 $\pm$ 4.45	71.02 $\pm$ 5.84	1.65	89	0.11
MMSE Values $\pm$ SD	29.07 $\pm$ 0.99	21.07 $\pm$ 3.56	-14.06	86	<b>0.001</b>
CDR	0 (0.00)	1 (0.00)	27.456	89	<b>0.001</b>
ADL	5.75 $\pm$ 1.22	7.93 $\pm$ 4.65	4.62	89	<b>0.001</b>
IADL	6.44 $\pm$ 2.01	12.52 $\pm$ 5.28	12.52 $\pm$ 5.28	85	<b>0.01</b>

Legend. AD = Alzheimer's disease, MMSE = Mini Mental State Examination. CDR = Clinical Dementia Rating. ADL = Activities of Daily Living, IADL = Instrumental Activities of Daily Living.

\*Significant results are in **BOLD**

Author Manuscript

Author Manuscript

Author Manuscript

Author Manuscript

**Table 2**

Whole and Hemisphere Superficial White Matter Group Comparisons

Region	Parameters	ANOVA		
		F	df	P
Whole	FA	3.292	2,90	<b>0.024</b>
	Axial	29.478	2,90	<b>0.001</b>
Brain	Radial	9.390	2,90	<b>0.001</b>
	MD	31.582	2,90	<b>0.001</b>

Legend. superficial white matter = Superficial White Matter; FA = Fractional Anisotropy; Axial = Axial Diffusivity; Radial = Radial Diffusivity; MD = Mean Diffusivity R = Right; L = Left.

\*Significant FDR corrected results are in **BOLD**

Author Manuscript

Author Manuscript

Author Manuscript

Author Manuscript